

***p*-shell hybridization and zero-field violation of Hund's rules: Engineering Hilbert spaces in artificial atoms**

Jordan Kyriakidis*

*Department of Physics and Atmospheric Science,
Dalhousie University, Halifax, Nova Scotia, Canada, B3H 3J5*

(Dated: May 23, 2019)

The magnetic-field dependence of many-body states in quantum dots can be tailored by controlling the mixing of various angular momenta. In lateral quantum dots—defined electrostatically in a two-dimensional electron gas—this mixing can be accomplished by introducing anisotropies in the confinement potential, thereby explicitly breaking rotational symmetry. Mixing can be severe enough to violate Hund's rules, even at zero magnetic field. We illustrate the principle through calculations of states and spectra of four-electron droplets (*p*-shell) with long-range Coulomb repulsions and confined in anisotropic potentials. Our results show that the Hilbert space in these nanostructures can be engineered to the particular application domain.

In order for quantum nanoelectronics to become a demonstrably viable technology, the particular nature of the discrete states of a finite system—a quantum dot, for example—must be both known and controlled. This is also a natural prerequisite for controlling the coherent time evolution of a nanoscopic quantum system.

In the present work, we study the specifics of particular quantum dots [1] defined electrostatically within a two-dimensional electron system (lateral quantum dots). By adjusting the shape of the confinement potential, individual many-body states within the quantum dots, and within the leads, may be tailored to exhibit a desirable magnetic-field dependence. (See, for example, Ref. 2.) Among similar lateral structures, the present dots have the distinguishing feature that the number of electrons can be controlled down to a single electron [1], similar to vertical devices [3]. They differ from vertical devices in that the confinement potential can be generally controlled to a greater degree; in the dots we study here, confinement is produced by four different gates. Because of this, singlet-triplet transitions [4] and negative differential resistance [5], for example, can be tuned at a *fixed* magnetic field by adjusting the gate voltage alone. Further, they differ from vertical devices in that the leads of lateral devices are the edges of a high-mobility two-dimensional electron gas (2DEG). In such devices, spin-splitting of the edge states, due primarily to exchange effects, results in a spatial separation of the spin channels. Consequently, the tunneling rates into and out of the quantum dot are measurably different for each spin species. This additional diagnostic tool has been recently used [6] to show how interactions force the collapse of the spin-singlet state at filling-factor $\nu = 2$.

The present lateral dots have a relatively small confinement energy ($\omega_0 = 1$ meV) compared to, say, vertical devices. Because of this, the system is more strongly interacting (Coulomb interactions $\sim \omega_0^{1/2}$, kinetic energy $\sim \omega_0$). This enhanced interaction strength largely drives the various phases we describe below. The dots are also anisotropic and, consequently, the many-body

states of the system contain mixed angular momenta. By studying the magnetic-field evolution of these states, their angular-momentum composition can be deduced.

The dots are well-isolated from the leads and we work in the Coulomb blockade regime; transport proceeds via single-particle sequential tunneling into and out of the quantum dot. We thus assume an isolated dot and look at its intrinsic properties.

Insight can be gained by looking first at the simple case of parabolic confinement. We first review the relevant spectra for dots containing four electrons. In these two-dimensional dots, the *s*-shell has one orbital with angular momentum $L_z = 0$ and the *p*-shell has two degenerate orbitals with angular-momentum $L_z = \pm 1$. Application of a magnetic field perpendicular to the 2DEG breaks the orbital degeneracy.

The noninteracting Hamiltonian is

$$H = \frac{1}{2m^*} \left(\mathbf{p} + \frac{e}{c} \mathbf{A}(\mathbf{r}) \right)^2 + \frac{1}{2} m^* \omega_0^2 r^2 + g\mu_B \mathbf{B} \cdot \mathbf{S}. \quad (1)$$

The single particle states are the well known [7, 8] Fock-Darwin states, or alternatively [9], and more useful in the present context, a set of two decoupled harmonic oscillators $|mn\sigma\rangle$:

$$E_{mn\sigma} = \hbar\Omega_+ \left(n + \frac{1}{2} \right) + \hbar\Omega_- \left(m + \frac{1}{2} \right) + g\mu_B B\sigma. \quad (2)$$

In this notation, the *z*-component of angular momentum of the state $|mn\sigma\rangle$ is $L_z = \hbar(n-m)$, *n* is the Landau-level index, and

$$\Omega_{\pm} = \frac{1}{2} \left(\sqrt{\omega_c^2 + 4\omega_0^2} \pm \omega_c \right), \quad (3)$$

with $\omega_c = eB/(m^*c)$ the cyclotron frequency and ω_0 the parabolic confinement frequency. We also take the magnetic field \mathbf{B} in Eq. (1), and throughout this paper, to be directed perpendicular to the two-dimensional plane of the dot. The final term in Eq. (2) is the Zeeman energy.

When more than one electron is trapped in the dot, long-range Coulomb repulsion plays a significant role,

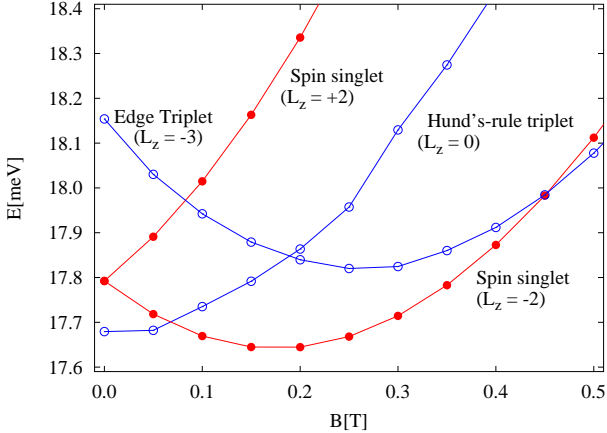


FIG. 1: Spectra for 2D parabolic dots containing four electrons with confinement $\omega_0 = 1$ meV. Only the lowest-lying states are drawn, showing the transitions to successive ground states. The states shown all have $S_z = 0$ and material parameters are for GaAs.

particularly for few-electron droplets, where screening is minimal and the long-range nature of the interaction is manifest. We take the full Coulomb interaction $V_C = e^2/|\mathbf{r}_1 - \mathbf{r}_2|$ and solve the problem numerically by exact diagonalization, exploiting the spin and rotational invariance of the model. (See Refs. [4, 10] for details.) Figure 1 shows the successive ground states for four particles, for GaAs. At zero field, the ground state configuration is a spin triplet with zero angular momentum. We label this state ‘‘Hund’s-rule state’’ because the dominant component, approximately 75%, of this correlated state is the Hund’s-rule state $|00 \downarrow, 00 \uparrow, 01 \downarrow, 10 \downarrow\rangle$ [11]. The first crossing occurs already below 0.1 T, and the new ground state is a spin singlet state with angular momentum $L_z = -2$. The dominant component of this state is the usual $\nu = 2$ state, $|00 \downarrow, 00 \uparrow, 01 \downarrow, 01 \uparrow\rangle$. Hence, this transition involves both a spin and an orbital transition. The second ground-state transition of relevance here, occurring at approximately 0.45 T, is to an ‘‘edge triplet’’ state. This is again a spin and orbital transition; the new ground state is a spin triplet and has angular momentum $L_z = -3$. The dominant contribution to this state is the single Slater determinant $|00 \downarrow, 00 \uparrow, 01 \downarrow, 02 \downarrow\rangle$. Continuing the magnetic field evolution would lead eventually to the $\nu = 1$ state, followed by fractional occupation of the lowest-Landau-level orbitals.

Just below 0.2 T, there is a transition between two *excited* states (see Fig. 1), both of which are triplets; one is the Hund’s-rule state, the other the edge triplet. Explicitly breaking the rotational (spatial) symmetry allows mixing between different angular-momentum states, but not different spin states. The edge triplet and Hund’s rule triplet are both strongly mixed near the transition [12].

The nature of the anisotropy in the confinement potential of the present dots has been explored in Ref. 4, where

the confinement potential has been found to fit very well the analytic form

$$V_{\text{con}} = \frac{1}{2}m^*\omega_0^2 \left[(x^2 + y^2) + \gamma \left(x - \frac{y^2}{D} \right)^2 \right]. \quad (4)$$

The gate geometry producing such confinement is sketched in the inset of Fig. 2. For the four-electron droplet, we find $\gamma = 0.5$ and $D = 5a_0$, where $a_0 = \hbar^2/(m^*e^2)$ is the effective Bohr radius. The first term in parentheses is the usual parabolic confinement, and the second term in parentheses is the explicit symmetry-breaking term which induces mixing in the angular momentum states. Because the anisotropy is of quartic order, non-zero matrix elements exist between states with angular momentum L_z and $L_z \pm \delta R$, where $\delta R = 0, 1, 2, 3, 4$. The respective Hilbert spaces of different *spin* angular momenta remain segregated.

It is useful to consider the Hamiltonian as two terms

$$H = H_0 + H_1. \quad (5)$$

H_0 contains the full Coulomb interactions, the kinetic energy, and the isotropic (parabolic) confinement potential, whereas H_1 contains only the anisotropic piece of the confining potential—the term proportional to γ in Eq. (4). We can label the eigenstates of H_0 as $|i, L_z, S\rangle$, which denotes the i -th state with z -component of angular momentum L_z , and spin S :

$$H_0|i, L_z, S\rangle = E_i^{(0)}(L_z, S)|i, L_z, S\rangle. \quad (6)$$

(In practice, we also use S_z as a good quantum number.) Figure 1 shows the field-dependence of several $E_i^{(0)}$.

The eigenstates $|j, S\rangle$ of the full anisotropic Hamiltonian H in Eq. (5) do not preserve angular momentum. These states can be constructed from the parabolic states $|i, L_z, S\rangle$:

$$|j, S\rangle = \sum_{i, L_z} \alpha_i^{L_z} |i, L_z, S\rangle. \quad (7)$$

The probability $P(L_z)$ that a given state $|j, S\rangle$ has angular momentum L_z is then given by

$$P(L_z) = \sum_i \left| \alpha_i^{L_z} \right|^2, \quad (8)$$

with the sum rule $\sum_{L_z} P(L_z) = 1$ conserving probability.

Our calculations of four interacting electrons in an anisotropic quantum dot, Eqns. (5), (4), proceed through two successive exact-diagonalisation procedures. In the first step, we compute the energy levels and eigenstates of four interacting electrons in a parabolic potential, H_0 in Eq. (5). As a basis, we use antisymmetrised four-electron states of the 2D harmonic oscillator (Fock-Darwin) states $|mno\rangle$. We use the full long-range Coulomb interaction,

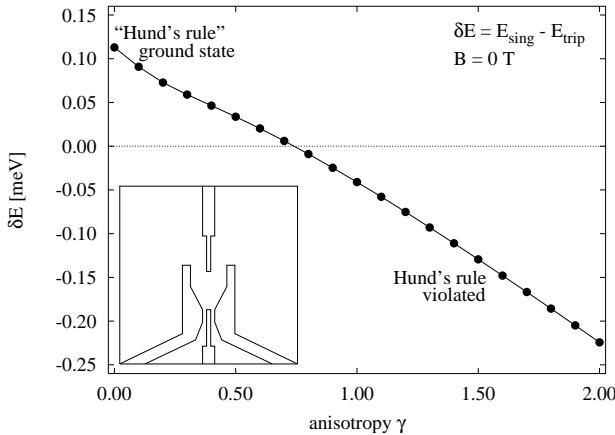


FIG. 2: Main plot: Zero-field violation of Hund’s rule. Plotted is the energy difference δE between the lowest-energy singlet and triplet states. Positive (negative) δE indicates a triplet (singlet) ground state. Inset: Sketch of the gate geometry producing anisotropic confinement, Eq. (4).

whose exact matrix elements are given in Ref. [4]. We ensure the accuracy of our results by progressively increasing the Hilbert space and monitoring the convergence of the energy levels. This yields the $E_i^{(0)}(L_z, S)$ and the $|i, L_z, S\rangle$ of Eq. (6).

In the second step, we diagonalise the full anisotropic Hamiltonian. The basis in this step is formed from the correlated eigenstates, $|i, L_z, S\rangle$, computed in the previous step. In this way, both the size of the Hilbert space and the degree of angular-momentum mixing can be controlled, and the convergence of the resulting energies and states can be readily investigated. Total spin S and z -component S_z are good quantum numbers and are used to classify our states.

We first discuss the zero-field case. Figure 1 shows a triplet Hund’s-rule ground state. This state has a filled s -shell and two singly-occupied p -orbitals. In contrast, the first-excited state is a singlet with a doubly-occupied s -orbital and one doubly-occupied p -orbital ($L_z = -1$). At zero field, the singlet is degenerate with its time-reversed partner—a doubly-occupied p -orbital with $L_z = +1$. Because the singlet state is degenerate and the triplet is not, we expect anisotropy to mix the singlet state more strongly than the triplet. As a consequence, the singlet-triplet gap should decrease as a function of anisotropy. (In other words, the lowest-energy triplet should rise faster in energy with anisotropy than the lowest-energy singlet.) This is indeed the case, as shown in Fig. 2. In essence, the anisotropy-induced p -shell hybridization is strong enough to produce two states delocalized across the $L_z = \pm 1$ orbitals. The splitting between these hybridized states is sufficient to overcome the exchange-energy savings associated with the triplet state. Hund’s rule is thus violated, even at zero magnetic field, and

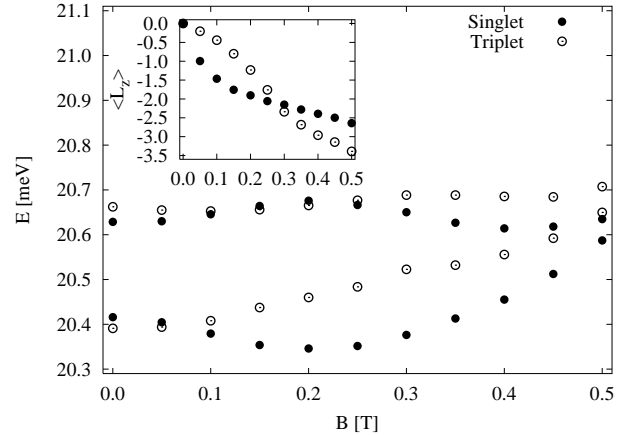


FIG. 3: Main plot: Energies of ground and first excited singlet and triplet states for the four-electron interacting droplet. The figure is for anisotropy parameters $\gamma = 0.5$ and $D = 5a_0$, and for $\omega_0 = 1$ meV. All other parameters are taken for GaAs. Inset: Average angular momentum $\langle L_z \rangle$ for the lowest-energy singlet and triplet states for the four-electron interacting droplet for the same set of parameters, as a function of magnetic field B [T].

the spin of the ground state can be tuned through the anisotropy.

In addition to the ground-state spin, the entire field-dependence of the many-body states can be tuned. The states analogous to those in Fig. 1 are shown in Fig. 3. The relatively weak field dependence of these states, is an indication of the angular-momentum mixing induced by the anisotropy. (Compare with Fig. 1 which shows states with definite angular momentum for the same energy interval (0.8 meV).)

The average angular momentum

$$\langle L_z \rangle \equiv \langle j, S | L_z | j, S \rangle \quad (9)$$

of the states shown in Fig. 3 are not constants but are themselves dependent on the magnetic field. This field dependence is shown in the inset of Fig. 3. At zero magnetic field, both states have $\langle L_z \rangle = 0$. This is a reflection of time-reversal symmetry, whose consequence is that the energy of each angular-momentum state depends on the magnitude, not the sign, of the angular momentum. Hence, $+L_z$ and $-L_z$ states are mixed equally. This degeneracy is lifted when time-reversal symmetry is explicitly broken, in favor of the negative angular-momentum states.

We focus first on the singlet. In the isotropic case, the lowest-energy singlet has $L_z = -2$. (See Fig. 1.) With the anisotropy present, the inset of Fig. 3 shows that $\langle L_z \rangle$ drops quickly from its zero-field value of $\langle L_z \rangle = 0$, and then, above 0.1 T, the field-dependence is much weaker, ranging from about $\langle L_z \rangle = -2$ to -2.5 . This indicates that the singlet state is primarily composed of the isotropic ($L_z = -2$) singlet state above a field of

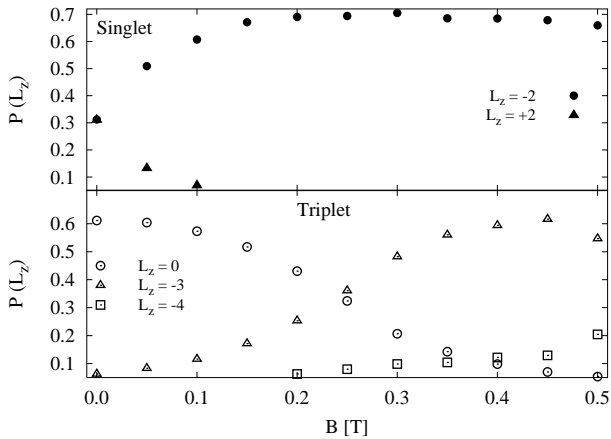


FIG. 4: Top: Dominant angular-momentum composition of the lowest-energy singlet state for the four-electron droplet. The figure is for anisotropy parameters $\gamma = 0.5$ and $D = 5a_0$, and for $\omega_0 = 1$ meV. The mixing occurs primarily at zero field. Many more angular-momentum states contribute to this state, but these all have less than 10% contribution. Bottom: Same plot, but for the lowest-energy triplet. In this case, the mixing occurs primarily at moderate (0.25 T) fields.

approximately 0.1 T. The angular-momentum mixing is more severe below this field value. These results are born out by further analysis. In Fig. 4, we plot the individual angular-momentum contribution, Eq. (8), for the singlet state. Only those angular momenta with $P(L_z) \geq 0.1$ are shown [13]. Figure 4 shows that, above 0.1 T, the isotropic $L_z = -2$ state is by far the dominant contribution; the contribution of its time-reversed partner, $L_z = +2$, dies out rapidly. Thus, the anisotropy does not severely mix angular momenta for this state above 0.1 T.

Figure 3 shows that the situation is rather different for the triplet state. Here $\langle L_z \rangle$ decreases qualitatively more uniformly than the singlet. In this case, significant mixing occurs between the edge triplet and the Hund's-rule state, also a triplet. (See Fig. 1.) In Fig. 4, we show the dominant angular momentum contributions to this lowest-energy triplet state, $P(L_z) \geq 0.1$. We see that the makeup of this state changes as a function of magnetic field, being composed primarily of the Hund's-rule state at low fields, and the edge triplet at fields above about 0.25 T. Another state, with $L_z = -4$, emerges above the background for fields greater than 0.3 T. Thus, the anisotropy induces significant angular-momentum mixing for the triplet state, although not at zero field.

Well-isolated quantum dots containing a known and small number of interacting electrons are simple enough to be amenable to a theoretical treatment through directly diagonalizing the relevant many-body Hamiltonian. By employing the successive exact-diagonalisation procedures outlined above, calculations can be extended with reasonable efficiency to anisotropic systems with

lower symmetry. At the same time, these systems are amenable to experimental analysis as well. With high source-drain spectroscopy, excited states as well as ground states can be directly imaged in experiment.

In the present work, we analyzed ground and excited states in a four-electron lateral quantum dot. We find that the (many-body) long-range Coulomb repulsion and the (single-body) anisotropic confinement potential both play important roles and both must be included in any analysis. By analyzing the magnetic-field dependence of these many-body levels, we have determined the average angular momentum of each level, which angular-momentum states are mixed together, how much they are mixed together, for both the ground and excited states of the system.

The interplay between experiment and theory can be exploited to design gate geometries which in turn produce confinement potentials whose magnetic field dependence can be predetermined to be as desired—a flat field-dependence, for example. These are the elements necessary to achieve quantum-state engineering, and a necessary prerequisite for controlling, in real time, the coherent time evolution of individual states that are robust towards decohering influences.

The author acknowledges discussions with Paweł Hawrylak. He is also grateful for the provision of unpublished experimental data from Andy Sachrajda. This work was supported by NSERC of Canada and by the Nanoelectronics Program of the CIAR.

* URL: <http://soliton.phys.dal.ca>

- [1] M. Ciorga, A. S. Sachrajda, P. Hawrylak, C. Gould, P. Zawadzki, S. Julian, Y. Feng, and Z. Wasilewski, Phys. Rev. B **61**, 16315 (2000).
- [2] A. Fuhrer, S. Lüscher, T. Heinzel, K. Ensslin, W. Wegscheider, and M. Bichler, Phys. Rev. B **63**, 125309 (2001).
- [3] L. P. Kouwenhoven, D. G. Austing, and S. Tarucha, Rep. Prog. Phys. **64**, 701 (2001).
- [4] J. Kyriakidis, M. Pioro-Ladrière, M. Ciorga, A. S. Sachrajda, and P. Hawrylak, Phys. Rev. B **66**, 035320 (2002).
- [5] M. Ciorga, M. Pioro-Ladrière, P. Zawadzki, P. Hawrylak, and A. S. Sachrajda, Appl. Phys. Lett. **80**, 2177 (2002).
- [6] M. Ciorga, A. Wensauer, M. Pioro-Ladrière, M. Korkusinski, J. Kyriakidis, A. S. Sachrajda, and P. Hawrylak, Phys. Rev. Lett. **88**, 256804 (2002).
- [7] V. Fock, Z. Phys. **47**, 446 (1928).
- [8] C. G. Darwin, Math. Proc. Cambridge Phil. Soc. **27**, 86 (1930).
- [9] Ł. Jacak, P. Hawrylak, and A. Wójs, *Quantum Dots* (Springer, Berlin, 1997).
- [10] A. Wensauer, M. Korkusinski, and P. Hawrylak, Solid State Commun. **130**, 115 (2004), cond-mat/0304275.
- [11] Our notation $|\cdots\rangle$ denotes appropriately antisymmetrised and normalised states.

- [12] In fact, there is a third triplet state (not shown) with $L_z = -1$ which, while comparable in energy, is not mixed strongly in the ground-state triplet.
- [13] The calculations were performed by mixing 31 different angular-momentum sectors, $L_z = -20$ to $L_z = +10$.